RSC Advances

Impact of Aluminium Addition on the Corrosion Behaviour of Sn-1.0Ag–0.5Cu Lead-free Solder

Journal:	*RSC Advances*
Manuscript ID	RA-ART-09-2015-018453.R1
Article Type:	Paper
Date Submitted by the Author:	21-Oct-2015
Complete List of Authors:	Mohd Said, Suhana; University of Malaya, Electrical Engineering Muhd Nordin, Nor Ilyana; University of Malaya, Mechanical Engineering Ramli, Rahizar; University of Malaya, Mechanical Engineering Weide-Zaage, Kirsten; University of Hannover, Mohd Sabri, Mohd Faizul; University of Malaya, Mechanical Engineering Mamat, Aizudin; University of Malaya, Mechanical Engineering Ibrahim, Syazana; MIMOS, Mainal, Azizah; University of Malaya, Chemistry Datta, Robi; University of Malaya, Electrical Engineering
Subject area & keyword:	Electronic materials < Materials

RSC Advances

PAPER

Impact of Aluminium Addition on the Corrosion Behaviour of Sn-1.0Ag–0.5Cu Lead-free Solder

Received 25th August 2015,
Accepted 00th September 2015

DOI: 10.1039/x0xx00000x

www.rsc.org/

N.I.M. Nordin[a], S.M. Said[b], R. Ramli[a], K. Weide-Zaage[c], M.F.M Sabri[a], A. Mamat[a], N.N.S. Ibrahim[d], A.Mainal[e] and R.S. Datta[b]

The effect of Al on the corrosion resistance behaviour of Pb-free Sn–1.0Ag–0.5 Cu–xAl solder (x = 0.2 wt.%, 0.5 wt.% and 1.0 wt%) in 5% NaCl solution was investigated by using potentiodynamic polarization and salt spray exposure. Passivation behaviour was evident in all the solder formulations containing Al, compared to the base SAC solder. FESEM and XRD results revealed that more dense passive films were formed on the solder containing Al, compared to the base solder. These passivation films contained intermetallic compounds such as Al_2O_3, $AlCuO_4$, SnO and SnO_2 served to prevent further reaction on the material surface. Polarization studies showed that the corrosion rate was 30% and 6% lower for alloys with 0.5 wt.% and 0.2 wt.% Al content, respectively, even though the corrosion potential shifted towards more negative values. The Al-added solder alloys exhibit more refined surface after exposure in the salt spray chamber and revealed no visible infiltration of aggressive ions at the solder–substrate joint. This work suggests a corrosion mitigation strategy for SAC 105 solder through doping of Al.

KEYWORDS: passivation, SAC105, Pb-free, solder, salt spray, NaCl, potentiodynamic

Introduction

The Restriction of Hazardous Substances (RoHS) implemented since 2007 became the market drive for the use of lead-free solders as interconnects in electronics circuits. So far, ternary alloys such as SnAgBi, SnBiZn, SnZnAl and SnAgCu have been proposed as viable lead-free alternatives. The main criteria for a solder alloys are high electrical and thermal conductivity, low electrical resistivity, low coefficient of thermal expansion (CTE), thermal fatigue resistance and cost effectiveness. The Sn–3.0Ag–0.5Cu (SAC305) alloy is a leading composition for lead-free solder alloys. The relatively high percentage of silver (Ag) in SAC305 results in a superior drop impact and thermal cyclic performance at the expense of increased cost. A solution to the problem is to develop a Sn–1.0Ag–0.5Cu (SAC105) alloy with relatively low Ag content, doped with a fourth element to improve the mechanical properties. For instance, minor addition of Zn and Bi creates a much superior SAC alloy owing to a higher creep resistance.[1,2] Moreover, the addition of Ni increase the shear strength at the joint.[3]

In previous work, Al-bearing SAC105 was shown to be advantageous in terms of its resistance against thermal aging, improvement of wettability and unaltered IMC thickness tested at high temperature. Consequently, despite the reactivity of Al as an individual metal, Al addition in low-Ag solder alloy improves some key characteristics of the material.[4–8]

Generally, solders are used as electronics packaging components in various applications, such as mobile electronics, automobile, and circuitry. Solders are subject to environmental degradation caused by humidity, weather, climatic condition, oceanic environment and thermal changes. The impact is twofold when solders are exposed towards air moisture and industrial contaminant, which often contain aggressive corrosion agents, such as sodium chloride (NaCl) ions. Solder materials must be studied for its resistance and behaviour towards such corrosion agents to be robust.[8,9] An immediate consequence is in our handheld gadgets, in which perspiration of consumers provides conductive and corrosive media, given that sweat contains a percentage of chloride at a low pH. The effect may range from being mild in a normal environment to critical in harsh environments. Various mechanical properties will significantly be affected after prolonged exposure to such corrosive environment. Naturally, corrosion is aggravated by the presence of chloride ions, which cause pit nucleation, the presence of humidity, which causes

[a] Department of Mechanical Engineering, University of Malaya, 50603 Kuala Lumpur, Malaysia
[b] Department of Electrical Engineering, University of Malaya, 50603 Kuala Lumpur, Malaysia
[c] RESRI Group Institute of Microelectronic Systems (IMS), Leibniz Universität Hannover, Appelstraße 4, 30167 Hannover, Germany
[d] Product Quality & Reliability Engineering (PQRE)Laboratory, Malaysian Institute of Microelectronic Systems(MIMOS) Berhad, Technology Park Malaysia, Kuala Lumpur 57000, Malaysia
[e] Department of Chemistry, University of Malaya, 50603 Kuala Lumpur, Malaysia
†Electronic Supplementary Information (ESI) available: See DOI: 10.1039/x0xx00000x

galvanic corrosion, and the dehydration (drying) phase, which traps chloride ions beneath the corrosion by-products. Corrosion rate is defined to be proportional to the metal etched per year (millimetre per year, mmpy). Uniform corrosion, pitting, galvanic and intergranular corrosion are all likely to happen to binary, ternary, quarternary and other compositions of solder alloys, which comprise more than a single metal. Galvanic mechanism is a possible occurrence because each metal has its own electrical potential, given that alloys are composed of a few metals. Thus, a solder alloy can be viewed as a collection of elements which are electrically connected, and its placement in an electrolyte will create potential differences. This condition will naturally create reduction and oxidation (redox) reaction, which is the basis of corrosion. Naturally, more reactive element within the composition will act as the anode, which preferentially corrodes quickly. Therefore, flow of electric current is generated, which continues until the potentials between both electrodes are equal.[10,11]

Lead-free solders are more susceptible to corrosion than leaded solders,[9] despite the fact that the main element in the solder alloys, i.e., tin (Sn), is known for forming a passivity film on its surface, and that the added elements, Ag and Cu, are acknowledged for their stable structures.[9,12,13] These elements react with each other and form intermetallic compounds (IMC) of the formula Ag_3Sn and Cu_6Sn_5. These compounds are well distributed in the matrix and at the interface of the solder–pad joint. Generally, IMCs are chemically stable and presumably insoluble in etchants, making them stable against corrosion. However, the nature of solder alloy, i.e., conductive and has multi elements, creates potential differences that eventually form a galvanic mechanism. Dissolution of Sn from solder matrix is accelerated by the presence of Ag_3Sn. The IMC possesses potential close to the potential value of Ag.[9,14,15] Reliability of solder joints is an important factor in choosing and shifting to lead-free solders. Table 1 provides the differences in potential that govern materials reactivity whilst in conductive mode.

Electronic products and assemblies are used in a variety of applications and subject to diverse extreme environment conditions. Specifically, a qualitative evaluation of the material's behaviour of reactivity under harsh condition is vital to evaluate an alternative solder alloy. In this work, the performance of SAC105 with minor addition of Al in the presence of aggressive ions (Cl^-) was investigated.

Experimental Procedures

Fabrication of Solder Balls and Assembly on Substrate

A lab-based apparatus was used to fabricate approximately 1 mm diameter solder balls. The substrate used was the copper pad with organic solderable preservative (OSP) surface finish. Surfaces of all substrates were thoroughly cleaned with isopropanol (IPA) for 30 s prior to attachment of solder balls. Figure 1 is showing the schematic of the solder to substrate attachment process. A reflow profile (Fig. 2) was used throughout the process.

Table 1 Galvanic Series of Commercial Metals in Seawater[10]

Metal	Electrode Potential,E^0 (V)	
Al	-1.66	Active/Anodic
Sn	-0.1375	
Cu	+0.34	
Ag	+0.7996	
Ag_3Sn	+0.7996	
AlCu		
Ag_3Al		Noble/Cathodic

Salt Spray Testing

The assembled solder/Cu OSP FR4 boards were positioned in the salt spray chamber. Three sets of boards for each composition were prepared, in which two sets were used for the examination of salt deposit after 24 and 96 h, whereas the other sets was assigned as control sample at initial condition. Examination of results involved inspection of surface degradation between solder compositions at different time of exposure to the salt mist. The cross section and solder–substrate joints of samples were investigated to determine the impact of exposure towards intermetallic growth.

Potentiodynamic Polarization

Gamry Potentiostat Reference 600 was used to assess the behaviour of all solder alloys tested in a 5 wt% NaCl solution. The potentiodynamic polarization was performed at scan rates of 2.0 mV/s. A three-electrode electrochemical cell system, with the mounted sample having an exposure surface area of 0.25 cm^2, was used as the working electrode. A platinum rod and a SCE were used as counter and reference electrodes, respectively.

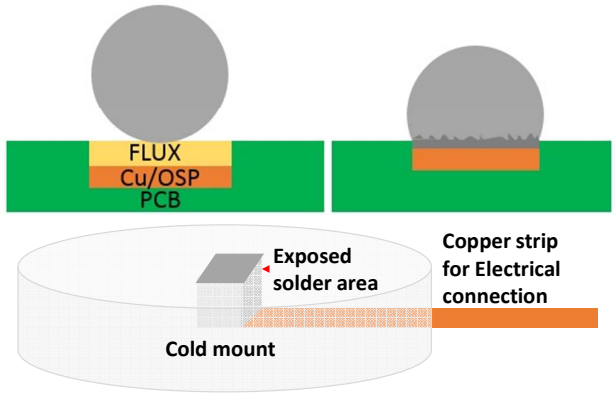

Fig. 1 Test samples for a) Attachment of solder balls to Cu/OSP substrate for salt spray testing b) Potentiodynamic polarization

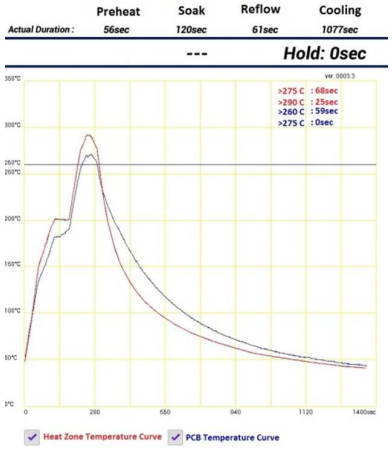

Fig. 2 Reflow profile for solder ball attachment on Cu/OSP pads

The scan potential ranged from −2.0 V SCE to 2.0 V SCE. Experiments were performed in Gamry Framework and analyzed in Gamry Echem Analyst. The software plotted the polarization curve and calculated the corrosion rate by using the following equation:

$$\text{Corrosion Rate, CR} = i_{corr}\frac{k.W}{AD} \quad (1)$$

where i_{corr} is the corrosion current (Amp), k is the constant which define the unit of corrosion rate, A is the surface area (cm^2), W is the equivalent weight (Table 2) and D is the density (7.32 g/cm^3). The samples were then subjected to a cycle of phase, microstructural, and elemental analyses to determine the evolution after potentiodynamic polarization in 5 wt% NaCl.

Analysis

As-mounted specimens and all tested samples were characterised using X-ray diffractometry (XRD) and field-emission scanning electron microscopy (FESEM). XRD analysis enables phase detection using a Bruker-AXS D8 diffractometer at 2θ values of 10° to 90° with Cu Kα radiation. A 40 kV voltage and a 30 mA current were applied to the X-ray tube. The high-score plus software was used to match the corresponding peaks with the standards from the International Committee of Diffraction Data (ICDD) XRD data file. FESEM (Zeiss Ultra-60) was used to examine the evolution of the surface microstructures. The elemental properties were characterised using an energy-dispersive X-ray (EDX) spectrometer attached to the FESEM.

Table 2 Weight and density for each composition of materials used in the test

	SAC105	With Al addition (wt%)		
		0.2	0.5	1.0
Eqv. Weight, gram	1.676	1.688	1.705	1.733
Density, g/cm^3	7.309	7.284	7.247	7.187

Results and discussions

Impact on Surface Morphology and Intermetallic Compounds

Cross section of the samples treated with 5 wt% NaCl was studied using FESEM. After 96 h of treatment, the surface of the solder spheres showed some degree of surface roughness at the exterior of all samples. Numerous corrosion pits and penetrated areas were observed, as seen in Figs. 3 to 5. Different incidences and patterns were observed on the surfaces of SAC105 and SAC105-xAl. The surface of both SAC105 and Al-added SAC105 were covered with a layer of mixed Sn, Cl and O, which suggest the formation of Sn–chloride and Sn–oxide layer that were discussed in previous studies.[19–22]

Visual inspection showed that superficial quality degradation of the Al-added alloys was less significant than the base alloy. Lead-free solders are known for its susceptibility towards corrosion owing to the inherent potential of dissimilar materials within the alloy compositions. In the case of Al added SAC105, Al generally forms a passive film, which is an aluminium oxide, on the surface. Nonetheless, the reaction is possible because the oxide film loses its stability since in chloride environment. Furthermore, localized corrosion takes place at the area where it is thermodynamically unstable, which acts as a seeding site for pitting corrosion.

Among the compositions of solder alloy used in this study, Al is the most anodic in the sequence of potentials (Sn<Ag<Cu<Al, see Table 1). Since Ag is the most cathodic, the potential difference creates instability within the Al atoms. This instability forces the element to form ions, thereby resulting in material disintegration from parts of the surface. Despite the general corrosion initiated by the conductive solution of NaCl, the material is exposed to intermetallic tension, which often

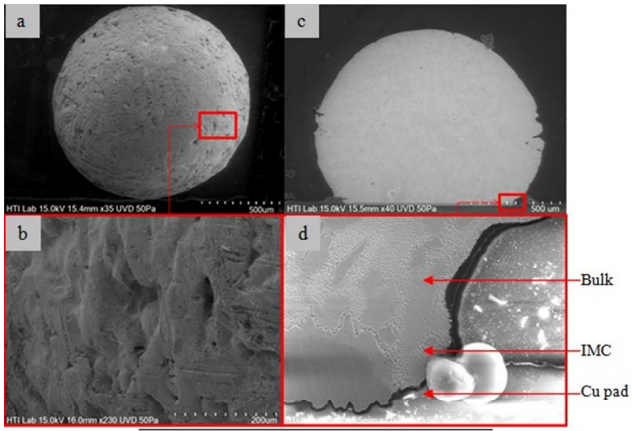

Element	Mass %
O	60.7
Sn	21.9
Cl	17.4

Fig. 3 SAC105 after 96 h of salt spray pre-conditioning: (a) surface morphology, (b) magnified surface, (c) cross section view and (d) magnified at joint.

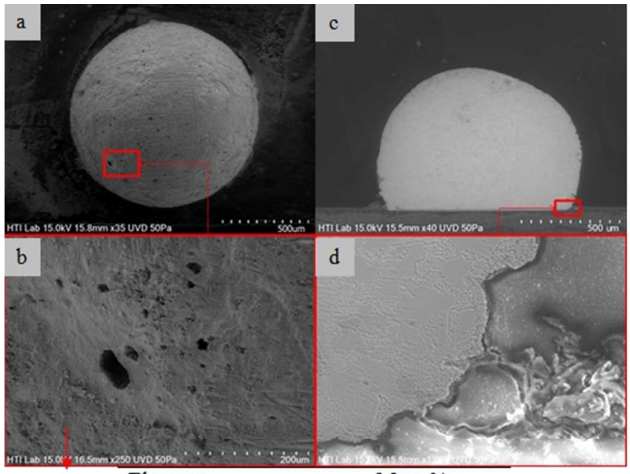

Element	Mass %
O	28.08
Sn	53.47
Cl	30.90

Fig. 4 SAC105–0.2 wt% Al after 96 h of salt spray pre-conditioning: (a) surface morphology, (b) magnified surface, (c) cross section view and (d) magnified at joint

lead to pitting, galvanic and intergranular corrosion. Hence, the numerous small holes due to material spalling were observed on the surface of alloys, as shown in Figs. 3(b), 4(b) and 5(b). Finer surface conditions were mostly seen for 0.2 wt% Al-added alloys, as seen in Fig. 4. By comparison, the alloy with 1.0 wt% Al displayed the most pitted surface.

The continuous oxidation and reduction reactions cause Sn to disintegrate from the solder matrix. However, less reactive components of the solder alloy, such as Ag_3Sn, $AlCu_2$, Ag_3Al and Cu_6Sn_5, remain in the matrix where it was initially located.[19,20] A previous study indicated that addition of 0.2 wt.% to 1.0 wt.% Al suppresses the formation of Ag_3Sn and Cu_6Sn_5, creates large number of Al–Ag, refines β-Sn dendrites and forms larger Al–Cu IMC particles.[23] Passivity loss leading to localised corrosion or pitting in passive metals is caused by a variety of different mechanisms.[24] Three main mechanisms discussed by most authors are penetration, film breaking and adsorption.[25]

This phenomenon could be related to the nature of the distribution of refined β-Sn dendrites and the Al–Cu particles within the solder bump. As mentioned before, the more noble metal forces the disintegration of weaker metal during the reduction process throughout the process of balancing the potential differences. In the current study, Ag and Ag_3Sn are less reactive than the other components within the solder alloy. Although Ag_3Sn was reduced with the addition of Al, the large potential difference between Al with Ag and Cu had created enough atom instability to induce material disintegration. This mechanism continues until the potential difference is balanced completely. Further information and characteristics of all materials are discussed and examined in the next section presenting the potentiodynamic polarization test, by which all materials were ranked based on their corrosive resistance.

The electrode potential of Ag_3Sn was proven to be close to Ag. The reaction that Ag_3Sn accelerates dissolution of Sn into corrosive medium from the solder matrix is well established.[12] Furthermore, Cu_6Sn_5, which was identified to form a fine inter-branch spacing, was suspected to provoke localized strain at the boundaries with the Sn-rich matrix. This feature could also be related to the susceptibility of this alloy to corrosion.[14]

The corrosion impact at the joint was monitored because the reliability of the material is important for electronics application. The addition of Al in SAC105 is more prone to pitting corrosion; this mechanism induces Cl^- ions to attack a localize area and continue to damage the adjacent inner material. The exact phenomenon involved alteration of microstructure, where it deforms the material. Specifically, the material is transformed from ductile to brittle at the location of the attack. This change in the microstructure of corroded regions may provide crack initiation sites, thereby decreasing the mechanical properties of the joints, because Al–oxides are hard particles, whereas Sn-chlorides are soft structures. Therefore, the inclusion of these components within the material after a certain period of material exposure to corrosive media is expected to influence the properties of the solder joint, specifically the mechanical behaviour, which is closely related to ductility. The FESEM images of the solder joint between SAC105 and the copper pad in Fig. 3(d), as well as for the Al added SAC105 in Figs. 4(d) and 5(d), revealed that the effect of corrosion on the alloys in 5% NaCl was harmless.

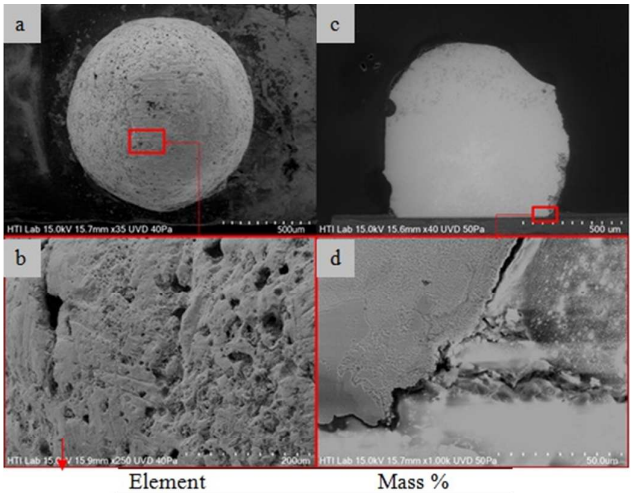

Element	Mass %
O K	38.3
Sn L	35.8
Cl L	26.0

Fig. 5 SAC105-1.0 wt% Al after 96 h of salt spray pre-conditioning: (a) surface morphology, (b) magnified surface, (c) cross section view and (d) magnified at joint

Polarization curve and corrosion rate in 5 wt% NaCl

Region AB corresponds to the cathodic reduction of H_20, which forms hydroxyl ions (OH^-). Further increase in potential up to point B resulted in sharp peak, which might be due to the dissolution of Al. The addition of OH^- ions to NaCl solution raised the anodic dissolution rate of Al. As shown in Table 1, Al is the most anodic, and thus it will be attacked preferentially by the OH^-. The Al content in the SAC105 alloy was varied from 0.2 wt% to 1.0 wt%. The polarization curves obtained for the alloys showed an active–passive transition at points A to B to C, followed by a transpassive region at points D to E.

The active dissolution of Al continues with increasing potential until the aluminate reached a critical value and supersaturates the surface of the alloy (point C in Fig. 6.). The SAC105 alloy with higher Al content showed strong tendency towards passivation, given that the passivation current density (i_p) were found to be lower than that of SAC105. The passivation behaviour was ascribed to the presence of SnO and $Sn0_2$ as well as the nature of Al to generate passivity film on the surface. Based on Fig. 6, the addition of 0.2 wt% Al results in a decrease in the corrosion current density (I_{corr}). However, addition of ≥0.5 wt% Al resulted in higher I_{corr}, as listed in Table 3. In addition, the corrosion potentials (E_{corr}) shifts towards more negative value. Similar to I_{corr}, a decrease in corrosion rate was observed for addition of 0.2 wt% Al, and the highest corrosion rate was found for alloy with 1.0 wt% Al (Table 3). The presence of Cl^- ion initiated crevice and pitting spots and was assumed to be responsible for the rupture of the passive layer at the breakdown potential (E_{BR}), which is approximately at −0.4mV vs. SCE. The E_{BR} values range around the same magnitude for all materials in this study.

By referring to the potentiodynamic polarization curve in Fig. 6, for SAC105 alloy and all of its variances with Al addition, the passivation process begins at −800 mV and extends to −400 mV vs. SCE, where the anodic current density never exceeds1 A cm^{-2}.

This is probably due to the formation of tin oxide (SnO_2),[21] which disappears at −400 mV when an abrupt increase of anodic current density occurred because of the breakdown of passive layers on the surface at E_{BR}. The incident of rapid increase of anodic current density results in an obvious x-direction of the curve. This corresponds to the active dissolution of Sn stimulated by the Cl^- ions, with the formation of soluble complexes of the type $SnCl_2$.[26] A point that should be noted, Sn is an anode in this electrochemical reactions and will always reacts with Cl^- to form $SnCl_2$, which is soluble in an aqueous solution.

The numerical data from the polarization curves of all materials were extracted and summarized in Table 3. At point D to point E, the current density slowly starts decreasing on further scanning in the anodic direction. When the potential increased, the current remains independent, thereby indicating the onset of a pseudo-passivation process, which is attributable to the formation of a corrosion film on the surface. At this point, this current is known as the pseudo-passivation current density, i_{pp}. As shown in Fig. 6, the i_{pp} values of all materials are in the range of 10 mA to 60 mA, while the pseudopassivation potential (E_{pp}) range extends from +200 mV to +600 mV vs. SCE. Moreover, the i_{pp} for SAC105 is approximately 0.2 mV higher than that of Al-added SAC105.

At point E, eminence performance had occurred in which the alloys with Al supersede SAC105. As observed, current density was not influenced by the increase in the trans-passivation potential for alloys with Al. For SAC105, the increase in trans-passivation potential increases the current density. This scenario is directly related to the passivation layer on the surface of the material during pseudo-passivation region. For SAC105, the increase in the trans-passivation potential induced shattering of the passivation layer, whereas for the Al-added SAC105, the layer persistently sticks on the surface until the scanning ends. This finding suggests that the formation of the oxide film on the surface had inhibited the reaction towards Cl^- ions. This oxide film is responsible for the suppression of the pitting corrosion for all Al-added SAC105 composition whilst protecting the larger part of the exposed area.

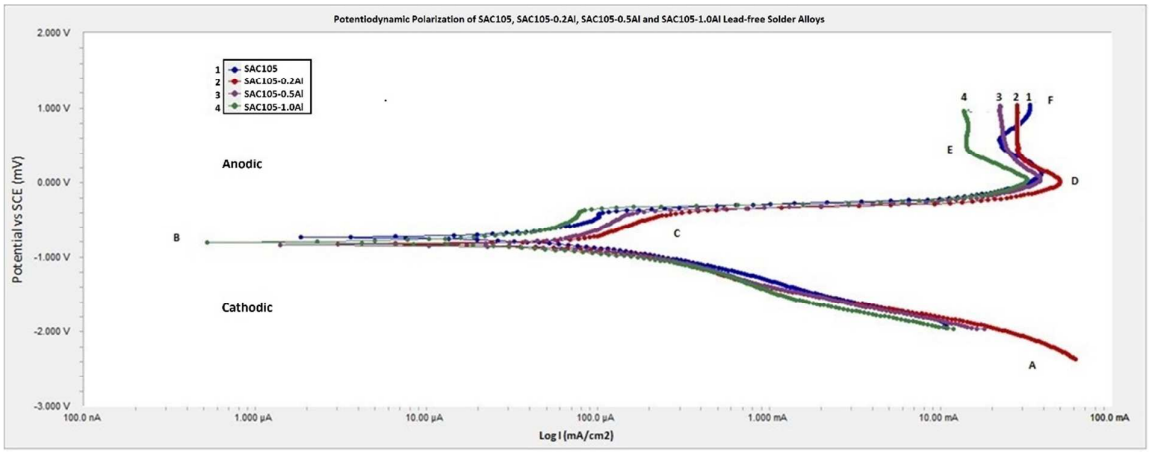

Fig. 6 Potentiodynamic polarization curves for SAC105 and SAC105-xAl

Table 3 Results for corrosion potential, current density and the corrosion rate

	E_{corr} (mV)	I_{corr} (μA)	Corrosion Rate(mmpy)
SAC105	−741.6	70.8	2.907
SAC105–0.2Al	−804.7	53.64	2.013
SAC105–0.5Al	−838.3	83.9	2.73
SAC105–1.0Al	−830.6	79.27	3.29

Impact of Aluminium Addition in SAC105 Solder Alloys

Through exposure in salt spray, all assembled samples exhibit tolerable and almost equal reaction towards Cl^- ions. In addition, examination at IMC has shown no visible crack caused by the penetration of Cl^-. However, the potentiodynamic polarization curves showed that Al-added SAC105 alloys are more reactive and have higher E_{corr}, which eventually lead to higher corrosion rate. Moreover, towards the end of the polarization, Al-added SAC105 solder alloys are more stable, in which the increase in voltage does not affect the current. This specific performance is best explained by Fig. 7. The Al-added SAC105 has more densely packed corrosion products on its surface, whereas SAC105 was covered with flake-like layer, which obviously offers numerous spots for attack from the aggressive Cl^-. The difference was ascribed to the additional layer of oxides, which are shown in Fig. 8. The inclusion of Al in SAC105 introduces oxide layers in the form of Al_2CuO_4 and Al_2O_3. These oxides layers add up to the surface protection provided by the major SnO and SnO_2. Thus, Al addition had altered the corrosion products on the surface of the solder alloy. The formed products offer better resistance towards the aggressive Cl^- through arrangement of firmer layers on the material surface to block from reaction with the corrosive agents in the environment.

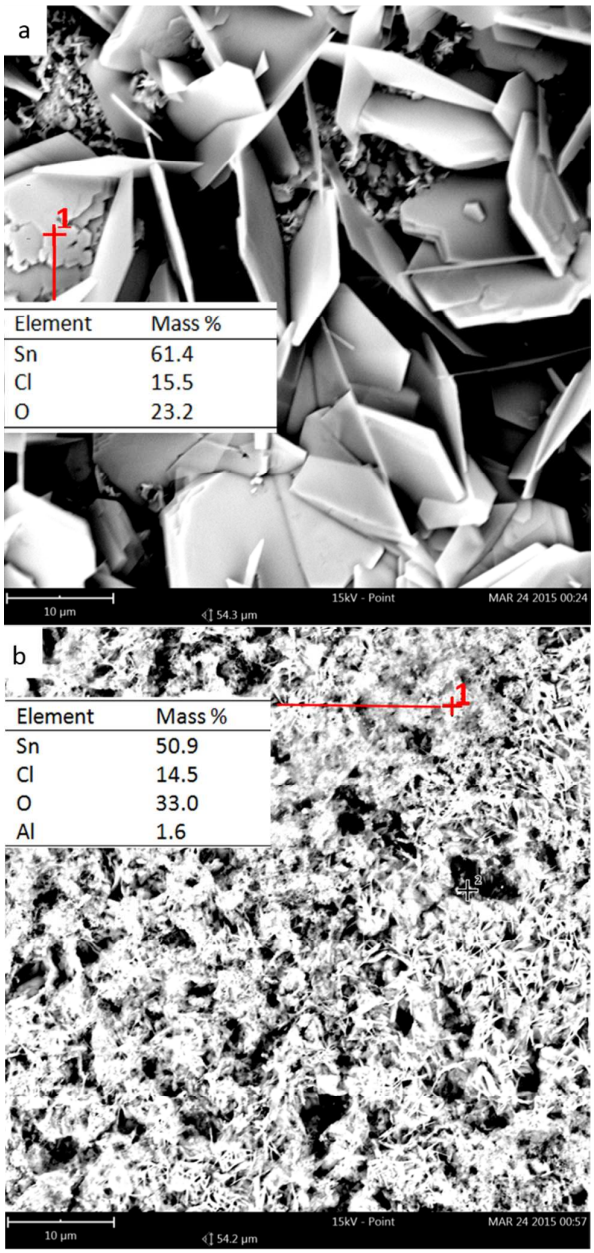

Fig. 7 Corrosion product on the surface of (a) SAC105 and (b) SAC105–1.0 wt% Al at point F of polarization plot.

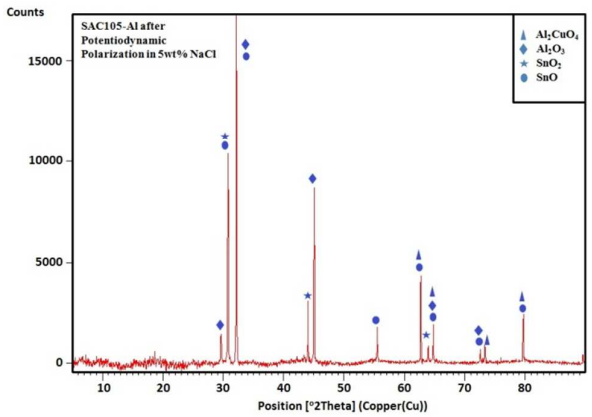

Fig. 8 Phases detected by XRD on the surface of SAC105–1.0 wt% Al

Conclusion

Results indicated that the addition of Al in the ternary SAC105 altered the corrosion product on the surface, thus indicating Al provides an enhanced passivation capability over the basic SAC105 solder alloy. The Al_2CuO_4 and Al_2O_3, together with the major SnO and SnO_2 formed on the surface decreased the susceptibility of the solder to corrosion. Exposure to 5% NaCl solution is an aggressive humidity acceleration test condition. In such a condition, corrosion of solder balls showed that the presence of Al protects the solder ball through the passivation layer. Three studies were done: salt spray, potentiodynamic polarization and morphology study. The visual inspection on salt sprayed samples showed that superficial quality degradation of the Al-added alloys was less significant than the SAC105. Corrosion was halted for all Al-added SAC105 as the material demonstrated table passivation during potentiodynamic test. The morphology study indicated there was no visible crack caused by the penetration Cl- aggressive ions. To conclude, the doping of Al in SAC solder serves as a corrosion mitigation strategy to the basic SAC 105 formulation.

Acknowledgements

The authors acknowledge financial support from University of Malaya under PPP (PG140-2014A) and UMRG (RP003D-13AET) grants.

References

1 M. Abtew , G. Selvaduray, J. Mater SciEng R, 2000,27,95-141
2 D.R. Frear, P.T. Vianco, J Metall. Mater Trans 1994,25(7),1509-1523.
3 J. Glazer, J Electron Mater, 1994,23,693-700.
4 S.K.Kang, A.K. Sarkhel, J Electron. Mater, 1994,23,701-707.
5 X. Deng, G. Piotrowski, J.J. Williams, N. Chawla, J Electron Mater, 2003,32(12),1403-1413
6 D.A. Shnawah, M.F.M. Sabri, I.A. Badruddin, J Microelectron, Electronic Components and Materials, 2012,42(2), 88 – 94.
7 L. Zhang, C.W. He, Y.H. Guo, J.G. Han, Y.W. Zhang, X.Y. Wang, J MicroelectronReliab,2012,52,559-578.
8 L. Dezhi, P.C. Paul, L. Changqing, J Corr. Sci, 2008,50,995-1004
9 B. Liu, T.K Lee, K.C. Liu, J Electron. Mater, 2011,40,2111-2118
10 M. G. Fontana and N. D. Greene, Corrosion Engineering, 2nd edition, McGraw-Hill, New York, 1978, 32.
11 G. Harsyanyi, J Microelectron. Reliab, 1999, 39, 1407-1411.
12 S. Fubin, L. Ricky, Proceeding of the 56th Electronic Components and Technology Conference, 2006, 891-898.
13 B.Y. Wu, Y.C. Chan, M.O Alam, J. Electrochem. Corr., J Materials Research, 2006, 21-62.
14 W.R. Osorio, L.C. Peixoto, L.R. Garcia, A. Garcia, J.E. Spinelli. J Electrochem Sci, 2012, 6436 – 6452.
15 SM. Hayes, N. Chawla, DR. Frear, J. Microelectron Reliab, 2009,49, 269–287
16 JESD22-A107B JEDEC. Salt Atmosphere 2004.
17 C.I. House, G.H. Kelsall, Electrochim. Acta, 1984, 29, 1459–1464.
18 V.S. Sinyavskii, V.V. Ulanova, V.D. Kalinin, J. Protection of Metals, 2004,40,481-490
19 A. Wierzbicka-Miernik, J. Guspiel, L. Zabdyr, Archives of Civil and Mechanical Engineering, 15(1), 206-213,
20 F. Rosalbino, E. Angelini, G. Zanicchi, R. Carlini, R. Marazza, Electrochim. Acta, 2009, 54, 7231–7235
21 S.S Abd El Rehim, M.Z. Ayman, F.M. Noble, J. Alloys and Comp, 2008, 424(1–2): 88-92.
22 X.L, Zhang, Corr. Sci, 2009, 51(3): 581-587.
23 D.A. Shnawah, S.M. Said, M.F.M. Sabri, I.A. Badruddin, T.G. Hoe, F.X. Che, A.N. Abood, J. Electron. Mater, 2012, 41(8): 2073-2082.
24 G.S. Frankel, J.Electrochem. Soc., 1998, 145, 2186–2198.
25 H. Bohni, Langmuir 3, 1987, 924–930.
26 M.N.Mohamed, N.A.Aziz, A.A.Mohamad, M.F.M.Nazer, J. Electron. Mater, 2015, 3: 28-32.

RSC Advances

PAPER